

---

**Molecular Basis of Cell and  
Developmental Biology:  
Acetylcholinesterase Dynamics at the  
Neuromuscular Junction of Live Animals**

Eric Krejci, Isabel Martinez-Pena y  
Valenzuela, Rafiq Ameziane and Mohammed  
Akaaboune

*J. Biol. Chem.* 2006, 281:10347-10354.

doi: 10.1074/jbc.M507502200 originally published online February 2, 2006

---

Access the most updated version of this article at doi: [10.1074/jbc.M507502200](https://doi.org/10.1074/jbc.M507502200)

Find articles, minireviews, Reflections and Classics on similar topics on the [JBC Affinity Sites](https://www.jbc.org/).

Alerts:

- [When this article is cited](#)
- [When a correction for this article is posted](#)

[Click here](#) to choose from all of JBC's e-mail alerts

This article cites 46 references, 24 of which can be accessed free at  
<http://www.jbc.org/content/281/15/10347.full.html#ref-list-1>

# Acetylcholinesterase Dynamics at the Neuromuscular Junction of Live Animals\*

Received for publication, July 11, 2005, and in revised form, February 1, 2006. Published, JBC Papers in Press, February 2, 2006, DOI 10.1074/jbc.M507502200

Eric Krejci<sup>‡</sup>, Isabel Martinez-Pena y Valenzuela<sup>§</sup>, Rafiq Ameziane<sup>§</sup>, and Mohammed Akaaboune<sup>§1</sup>

From the <sup>§</sup>Department of Molecular, Cellular, and Developmental Biology and Neuroscience Program, University of Michigan, Ann Arbor, Michigan 48109 and <sup>‡</sup>INSERM U686, Biologie des Jonctions Neuromusculaires, 45 Rue des Saints Pères, 75006 Paris, France

At cholinergic synapses, acetylcholinesterase (AChE) is critical for ensuring normal synaptic transmission. However, little is known about how this enzyme is maintained and regulated *in vivo*. In this work, we demonstrate that the dissociation of fluorescently-tagged fasciculin 2 (a specific and selective peptide inhibitor of AChE) from AChE is extremely slow. This fluorescent probe was used to study the removal and insertion of AChE at individual synapses of living adult mice. After a one-time blockade of AChEs with fluorescent fasciculin 2, AChEs are removed from synapses initially at a faster rate ( $t_{1/2}$  of ~3 days) and later at a slower rate ( $t_{1/2}$  of ~12 days). Most of the removed AChEs are replaced by newly inserted AChEs over time. However, when AChEs are continuously blocked with fasciculin 2, the removal rate increases substantially ( $t_{1/2}$  of ~12 h), and most of the lost AChEs are not replaced by newly inserted AChE. Furthermore, complete one-time inactivation of AChE activity significantly increases the removal of postsynaptic nicotinic acetylcholine receptors (AChRs). Finally, time lapse imaging reveals that synaptic AChEs and AChRs that are removed from synapses are co-localized in the same pool after being internalized. These results demonstrate a remarkable AChE dynamism and argue for a potential link between AChE function and postsynaptic receptor lifetime.

In cholinergic synapses, AChEs<sup>2</sup> play a critical role in terminating synaptic transmission by hydrolyzing the neurotransmitter acetylcholine (1). At the neuromuscular junction (NMJ), AChE tetramers are specifically clustered in the basal lamina by collagen Q (ColQ) (2). The ColQ contains two heparin binding domains (3) that interact with heparan sulfate proteoglycans, such as perlecan (4, 5), which in turn interacts with dystroglycan (6, 7). In ColQ, perlecan, and dystroglycan null mice, AChE is not clustered at the NMJ (5, 8, 9). In addition, mutations in the C-terminal domain of ColQ impair AChE accumulation in congenital myasthenia syndrome patients (3, 10) and prevent the interaction of ColQ with muscle-specific tyrosine kinase (11). Although much work has been devoted to the molecular characterization of AChE, little is known about how this enzyme is maintained and regulated at single mature synapses *in vivo*.

Previously, a few studies have attempted to investigate the turnover of AChE at the NMJ. Most of these studies have relied upon analysis by an

indirect method using a radioactively labeled ligand. The AChE half-life was then inferred from measurements by comparing the amount of AChE insertion into synapses in entire muscles at various times after initial saturation. These studies suggest that AChEs are very stable in the basal lamina ( $t_{1/2}$  around 20 days) (12, 13). In this work, we sought to study AChE dynamics more directly using fluorescence imaging techniques by assaying the intensity of fluorescently-tagged fasciculin 2 at individual junctions in living mice. Fasciculin 2 is a toxin isolated from the green mamba snake (14) and belongs to the same family as  $\alpha$ -bungarotoxin, the selective AChR blocker (16). Fasciculin 2 has very high affinity for AChE, similar to the binding of  $\alpha$ -bungarotoxin to nicotinic receptors (17). Previously, radiolabeled fasciculin 2 has been used to quantify AChE density at the NMJ (18). More recently, fluorescent fasciculin 2 has been used to label AChE on cultured cells, on fixed muscle (4), and in living synapses (19).

In this work, we show that the interaction between fluorescently-tagged fasciculin 2 and AChE is strong enough to be used as a powerful tool to study AChE dynamics in living synapses. We demonstrate that synaptic AChE removal is dependent upon its blockade with fasciculin 2, and blockade of AChE results in a profound decrease in AChR half-life. Removed AChEs from synapses are in most cases co-localized with AChRs in the same intercellular compartments.

## MATERIALS AND METHODS

**Animals**—Non-Swiss Albino mice (6–10-week-old females, 20–25 g) used in this study were obtained from Harlan Sprague-Dawley (Indianapolis, IN).

**Toxins**—Fasciculin 2 was purchased from Latoxan and conjugated by Molecular Probes, Inc. (Eugene, OR). Conjugation and purification of fasciculin 2 with the Alexa 594 dye was performed in 1 M sodium bicarbonate buffer (pH 8.3) by dissolving the succinimidyl ester of the dye in aqueous media as described by Panchuk-Voloshina *et al.* (20). The conjugate fasciculin 2 Alexa dye was purified from unconjugated dye by size exclusion chromatography using Bio-Gel P-30 (Bio-Rad), with or without a small addition of Toyopearl HW-40 (TosoHaas, Montgomeryville, PA). The dye attached to one or more lysine residues in the protein at the ratio of 1.5 mol of Alexa 594 attached/mol of fasciculin 2.

We also derived biotinylated toxin by incubating fasciculin 2 with NHS-XX-Biotin (Sigma) in 20 mM Hepes, pH 7.0. The ratio of biotin to fasciculin 2 was found to be 2:1. The unincorporated biotin was eliminated by using a NAP5 column (Amersham Biosciences). Labeled and unlabeled bungarotoxin were purchased from Molecular Probes.

**Biochemical Analysis of the Labeled Toxin**—Supernatant of COS cells transfected with Rat AChE cDNA was mixed with conjugated or unconjugated fasciculin 2 in 50 mM potassium phosphate buffer (pH 7.4) for 1 h at room temperature. AChE activity was then determined by the Ellman method. The mix was incubated with acetylthiocholine (0.5 mM) and DTNB (0.75 mM), and the yellow color variation was monitored with a plate reader (Bio-Rad) at 415 nm over time. A curve of AChE

\* This work was supported by the University of Michigan, NINDS, National Institutes of Health, Grant NS047332 (to M. A.), and CNRS, AFM, and la Fondation pour la Recherche Médicale (to E. K.). The costs of publication of this article were defrayed in part by the payment of page charges. This article must therefore be hereby marked "advertisement" in accordance with 18 U.S.C. Section 1734 solely to indicate this fact.

<sup>1</sup> To whom correspondence should be addressed: Dept. of Molecular, Cellular and Developmental Biology, University of Michigan, 830 N. University Ave., Ann Arbor, MI 48109. Tel.: 734-647-8512; Fax: 734-647-0884; E-mail: makaabou@umich.edu.

<sup>2</sup> The abbreviations used are: AChE, acetylcholinesterase; AChR, acetylcholine receptor; ColQ, collagen Q; NMJ, neuromuscular junction; CHAPS, 3-[(3-cholamidopropyl)dimethylammonio]-1-propanesulfonic acid; TEMED, *N,N,N',N'*-tetramethylethylenediamine; DFP, diisopropylfluoro phosphate.

## AChE Turnover in Vivo

activity inhibition in the presence of conjugated and unconjugated fasciculin 2 was then generated (Fig. 1A).

**Encapsulated Enzyme**—Mouse brain was homogenized in 10 ml of cold buffer solution (20 mM Hepes, pH 7.4, 10 mM EDTA, 0.154 M NaCl, 2 mM benzamidine) and centrifuged for 30 min at  $18000 \times g$ . The pellet was then solubilized in 1 ml of cold buffer solution containing 1% CHAPS as detergent. This crude detergent extract was mixed with acryl-bisacrylamide (10% final concentration), ammonium persulfate and TEMED were then added, and the mix was poured into a calibrated 50- $\mu$ l siliconed glass capillary. Immediately after polymerization, the gel was expelled and cut into 4.5-mm fragments (corresponding to 3  $\mu$ l of gel). Butylcholinesterase activity was irreversibly blocked by incubating the fragments in phosphate buffer containing  $5 \times 10^{-5}$  M tetra(monoisopropyl)pyrophosphortetramide for 16 h (20) and then washed out with phosphate buffer. To measure initial AChE activity, each fragment was individually put into the wells of a microtitration plate and bathed with 100  $\mu$ l of Ellman solution for 3 min or 10 min on a plate mixer; the supernatant of each well was transferred into the well of a new plate with a multichannel pipette, and the well containing the gel was covered with 100  $\mu$ l of phosphate buffer for 10 min to wash the yellow product resulting from the enzymatic reaction that still remained in the gel. The 100  $\mu$ l of washing solution was then mixed with Ellman's solution, and the OD at 415 nm was measured using a microplate reader (Bio-Rad). After measuring AChE activity, the fragments were incubated for 3 h with 1  $\mu$ M conjugated or unconjugated fasciculin 2. The gels were washed twice with 100  $\mu$ l of phosphate buffer for 15 min, and the activity was measured again to be sure that all AChE activity was blocked (as described previously), and the fragments were incubated with 100  $\mu$ l of phosphate buffer for the duration of the experiment. For example, after 1 day, the phosphate buffer was collected, and recovery of AChE was measured as described above. The  $\Delta$ OD/min for each fragment was measured and normalized to gel controls that were not incubated with fasciculin 2. The same procedure was repeated for each data point (from 1 to 7 days). Each point represents the mean of three fragments, and the experiment was reproduced with independent extracts from mouse brain. We initially tried this experiment with the collagen-tailed forms of AChE from mouse muscle extract, but the concentration of AChE in the crude extract is too low to be reliable for measuring AChE activity.

**In Vivo Imaging of Neuromuscular Junctions**—The techniques of animal preparation, sternomastoid muscle presentation, and neuromuscular imaging used in this work have been previously described in detail (21). For this study, mice were anesthetized with an intraperitoneal injection of ketamine and xylazine (17.38 mg/ml). The anesthetized mouse was placed on its back on a customized microscope stage, and synapses were viewed through neutral density filters under an automatic programmable controller using a water immersion objective ( $\times 20$  universal apochromate, 0.7 numerical aperture Olympus BW51; Optical Analysis Corp.) and a digital CCD camera (Retiga EXi, Burnaby, Canada). When animals were monitored over days, the incision was sutured after each session, and the animal was allowed to fully recover before the next imaging session.

**Quantitative Fluorescence Microscopy**—The intensities of fluorescent bungarotoxin bound to AChR and fluorescent fasciculin 2 bound to AChE at neuromuscular junctions were assayed using a quantitative fluorescence imaging technique that was developed by Turney and colleagues (22, 23), which relies on ratiometric comparisons of fluorescence intensity at synapses with the intensity of a nonbleaching inorganic fluorescence polymer concurrently viewed with the same optical system. This technique compensates for spatial and temporal variations in image brightness due to the light source, microscope, and camera and

therefore permits analysis of changes in fluorescence intensity (*i.e.* number of fluorescent molecules) during and between imaging sessions over any time interval. Image analysis was performed using IPLAP (Sacana-tytic) or Matlab (Mathworks).

**Single Saturating Dose of Alexa 594 Fasciculin 2**—To ascertain the dose of fluorescent fasciculin 2 necessary to saturate all AChE binding sites *in vivo*, we generated a standard curve of AChE saturation with fluorescent fasciculin 2, and we found that all AChEs were saturated after applying a concentration of 7  $\mu$ g/ml fluorescent fasciculin 2 to the sternomastoid of the mouse for 3 h. To be sure that all AChE molecules had been saturated with fasciculin 2-Alexa 594, a second fluorescently labeled fasciculin 2 (fasciculin 2-Alex 488) was added to the sternomastoid muscle, and synapses were imaged. The absence of green labeling indicated that the original Alexa 594 fasciculin 2 adequately saturated all AChE molecules. The loss of AChE was then monitored over time with or without saturating AChRs with a single application of  $\alpha$ -bungarotoxin (5  $\mu$ g/ml, 1.5 h). We and others have shown that the dose of bungarotoxin used in this study is sufficient to silence postsynaptic response (24–27).

**Insertion of AChE**—To test whether the loss of AChE that occurs following saturation of the NMJ with fluorescent fasciculin 2 is matched by a corresponding insertion of new AChE, AChEs were saturated with fasciculin 2-Alexa 594 (7  $\mu$ g/ml, 3 h), and the nonbound Alexa 594 fasciculin 2 was washed out continuously with lactated Ringer's for 15–20 min. The first views of superficial NMJs were imaged, the wound was sutured, and the animal was allowed to recover in a heat chamber. From 1 to 7 days later, the animal was anesthetized, sternomastoid muscle was exposed, and the same synapses were reimaged to assay the loss of fluorescence intensity. At each time point, AChEs were then saturated a second time with new fresh fasciculin 2-Alexa 594, and fluorescence intensity was again assayed.

**Chronic Blockade of AChE with Fasciculin 2-Alexa 594**—To assay the effect of continuous AChE blockade on AChE loss rate, the sternomastoid muscle was saturated with fasciculin 2-Alexa 594 (7  $\mu$ g/ml for 3 h), and superficial synapses were imaged. We then maintained the AChE blockade by adding new fresh fasciculin 2-Alexa 594 (7  $\mu$ g/ml) to the neck every 2 h for the duration of the experiment (8 h). In this way, AChE activity was continuously blocked with fasciculin 2-Alexa 594. During the experiment, animals were reanesthetized and intubated with an artificial respirator. These experiments could not be carried out for more than 8 h because of mortality, presumably due to the blockade of synaptic transmission. At the end of the experiment, the muscle was washed out continuously with lactated Ringer's for 15–20 min, and then the same synapses were relocated and imaged, and their fluorescence intensity was assayed.

**Effect of AChE Inhibition on Postsynaptic AChR Removal**—To determine the effect of AChE inhibition on the removal rate of postsynaptic AChRs, the sternomastoid muscle was labeled with a low dose of Alexa 594 bungarotoxin (5  $\mu$ g/ml for 2 min; Molecular Probes), so synaptic transmission remained fully functional. After waiting 1–2 days to allow clearance of unbound fluorescent bungarotoxin, superficial synapses were imaged, and then a single saturating dose of fasciculin 2 (7  $\mu$ g/ml, 3 h) was added to the sternomastoid muscle to block AChE activity. Three days later, superficial neuromuscular junctions that had been labeled with fluorescent bungarotoxin were reimaged, and their fluorescence intensities were measured.

**Confocal Microscopy**—The sternomastoid muscle of normal and denervated mice (8–10 days after nerve axotomy) was doubly labeled with fasciculin 2-Alexa 594 (to label AChE) and Alexa 488 bungarotoxin (to label AChR). 3–6 days after initial labeling, synapses were imaged

using *in vivo* fluorescence imaging or confocal microscopy. The analysis of intracellular co-localization of AChE/AChR was carried out using oil immersion lenses and laser illumination on an Olympus FV500 confocal microscope. A series of optical planes were collected in the *z* dimension (*z*-stack) and collapsed into a single image. One *z*-stack image was chosen to show the intracellular colocalization of AChR and AChE. Images presented under "Results" were produced and adjusted for brightness and contrast using Adobe Photoshop 8.

## RESULTS

**Use of Fluorescent Fasciculin 2 as a Probe for Studying AChE Dynamics in Vivo**—In this study, we first tested whether fluorescent fasciculin 2 can be used as a probe to label AChE in living animals and if it is suitable for studying the dynamics of AChE *in vivo*. To this end, the sternomastoid muscle of an anesthetized mouse was labeled with fasciculin 2-Alexa 594 (2  $\mu\text{g}/\text{ml}$ ); after only a 30-min incubation with fluorescent toxin, synapses were bright enough to be readily imaged. The saturation of all AChEs was then achieved by applying a concentration of 7  $\mu\text{g}/\text{ml}$  fasciculin 2-Alexa 594 for at least 3 h to the neck of the mouse.

To determine the specificity of fluorescent fasciculin 2 labeling at synapses *in vivo*, the sternomastoid muscle was saturated with unconjugated fasciculin 2 (7  $\mu\text{g}/\text{ml}$ , 3 h) or a specific AChE inhibitor BW284C51 (10 mg/ml, which competes with fasciculin 2). When fasciculin 2-Alexa 594 was then added to the muscle, no fluorescent signal was detected at synapses. In addition, the labeling of AChE with fluorescent fasciculin 2 was absent in ColQ<sup>-/-</sup> mutant mice in which AChEs fail to cluster at synapses (28). These results indicate that fluorescent fasciculin 2 labels only when AChE binding sites are available.

To determine whether conjugation of fasciculin 2 with Alexa dye modifies the binding properties of the toxin, recombinant AChE was mixed with conjugated or unconjugated fasciculin 2, and the inhibition curves were compared (Fig. 1A). A small shift to the right (corresponding to a decrease in affinity) was observed for conjugated fasciculin 2; however, at a concentration of 10 nM (70 ng/ml), almost all AChE activity was inhibited by both conjugated and unconjugated fasciculin 2, leaving only residual activity, as previously described (29). This result indicates that conjugation of the toxin with Alexa dyes does not significantly modify its properties.

To monitor spontaneous AChE-fasciculin 2 dissociation, we followed the apparent unbinding of fluorescent fasciculin 2 both *in vitro* and *in vivo*. Mouse brain extracts containing a high concentration of AChE tetramers (100 nM) were encapsulated into a gel, which was then cut in small fragments and incubated with conjugated or unconjugated fasciculin 2. After a 3-h incubation with 7  $\mu\text{g}/\text{ml}$  conjugated or unconjugated fasciculin 2, AChE activity was inhibited, and only residual activity was detected, as described previously (29). AChE activity recovery (presumably due to the apparent fasciculin 2 dissociation from AChE) was then measured over 7 days. At each time point, the phosphate buffer was replaced with a fresh buffer. After 7 days, only a very slow recovery of AChE activity was detected in both conjugated (corresponding to recovery a half-time of  $\sim 15$  days) and unconjugated fasciculin 2 ( $t_{1/2}$  more than 20 days) (Fig. 1B).

The apparent dissociation of AChE-fluorescent fasciculin 2 at the NMJ was then assessed *in situ*, where the concentration of AChE is estimated to be very high ( $\sim 0.2$  mM) (18). First we tested whether the saturation of AChE by fluorescent fasciculin 2 is achieved in fixed and living synapses under the same labeling conditions. To do this, fixed and living sternomastoid muscles were labeled with fasciculin 2-Alexa 594 (7  $\mu\text{g}/\text{ml}$ , 3 h) to saturate all AChE binding sites. To ensure that all

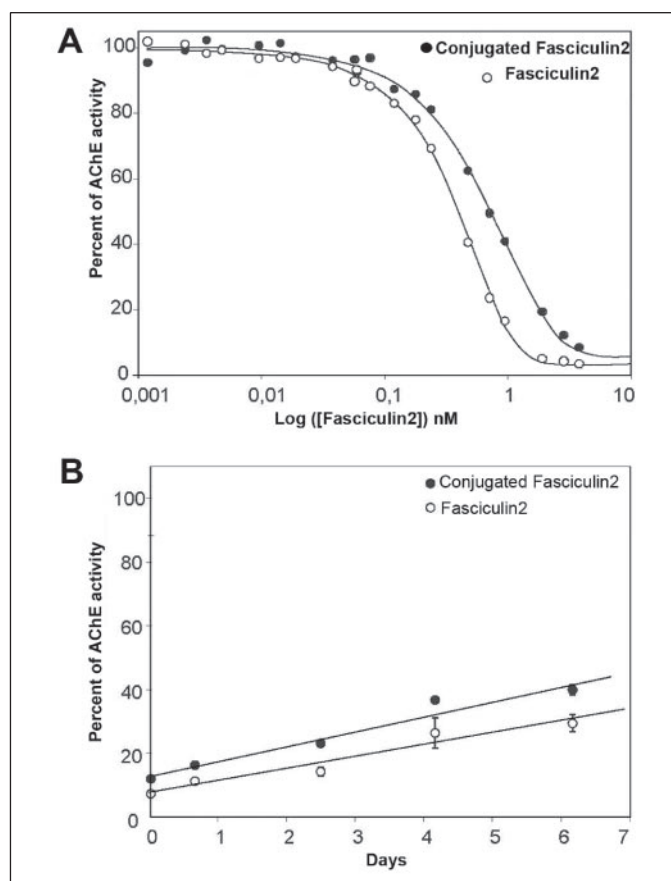


**FIGURE 1. Inhibition of AChE activity with conjugated fasciculin 2.** A, dose-response curve of AChE inhibition by conjugated and unconjugated fasciculin 2. Recombinant monomeric Rat AChE was incubated with different concentrations of unconjugated and conjugated fasciculin 2 for 1 h. Note that more than 94% of AChE activity was inhibited by both unconjugated and conjugated fasciculin 2, consistent with previous reports (29). B, evolution over time of AChE activity after inhibition with conjugated and unconjugated fasciculin 2. Brain extract in acrylamide gel was incubated with unconjugated and conjugated fasciculin 2 (1  $\mu\text{g}/\text{ml}$ ) for 2 h. The AChE activity of each fragment was measured over time and normalized to initial values of each sample and to the activity of noninhibited enzyme. The plots represent the mean of three gels. We observed a small recovery of AChE activity over 7 days. However, in the control gel, AChE activity remained constant.

AChEs were saturated by fasciculin 2-Alexa 594, a dose of fluorescently labeled (green) fasciculin 2-Alexa 488 was applied. No green fluorescence signal was observed after this labeling. This result indicates that the same level of maximal binding occurs in both fixed and living tissue. To assay the dissociation of fluorescent fasciculin 2-AChE, fixed muscle was saturated with fasciculin 2-Alexa 594, and superficial synapses were then imaged, and the loss of fluorescence was monitored over time using the same procedure that was used to label synapses *in vivo*. After 7 days, we found that the decrease in fluorescence was only  $10 \pm 3.9\%$  (S.D.,  $n = 20$ ) of original fluorescence (Fig. 2C). Similar results were obtained when the sternomastoid muscle was first fixed with 2% paraformaldehyde, saturated with fluorescent fasciculin 2, and then transplanted into the neck of a host mouse. After 7 days, we found that the loss in fluorescence was only  $\sim 15\%$  ( $n = 6$ ) at the NMJs ( $t_{1/2}$  of loss  $\sim 30$  days) (Fig. 2, B and C), indicating that the rapid loss of fluorescent fasciculin 2 from the surface of synapses *in vivo* (see below) is not due to biological processes that occur at the surface of the NMJ. Altogether, these results suggest that the  $k_{\text{off}}$  of fasciculin 2 is slow at the NMJ.

Whereas the above controls suggest that fasciculin 2-Alexa 594 has a strong affinity for AChE, we were surprised to find that unconjugated fasciculin 2 can displace conjugated fasciculin 2. Living or fixed synapses

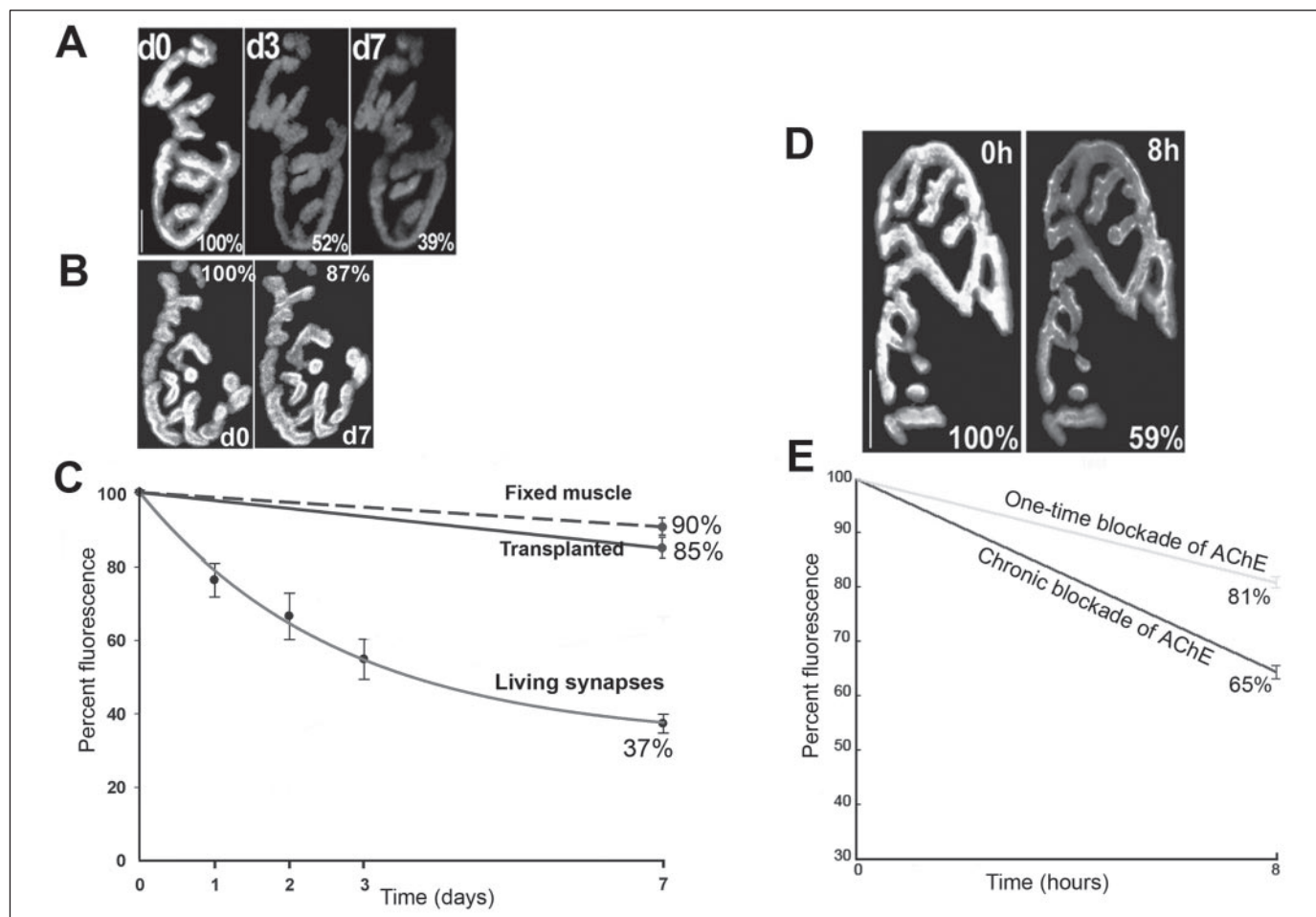


**FIGURE 2. AChE loss from and insertion into the NMJ of living mice.** *A*, example of a mouse neuromuscular junction that was measured three times over 7 days. The total fluorescence intensity of fasciculin 2-Alexa 594 was expressed as 100% at the time of saturation and determined on each successive view by comparing it with the fluorescence intensity of a nonbleaching standard (22). Pseudocolor images provided a linear representation of the density of AChE (white-yellow, high density; red-black, low density). Scale bar, 20  $\mu\text{m}$ . *B*, example of a fixed synapse that was labeled with fasciculin 2-Alexa 594 and measured twice over 7 days. *C*, graph summarizes results obtained from all junctions with the approach shown in *A* and *B*. Each data point represents the mean percentage of fluorescence intensity  $\pm$  S.D.; e.g., 23% of AChEs are lost in the first 24 h. The loss of remaining fluorescently tagged fasciculin 2 slowed progressively on subsequent days, and the residual fluorescence intensity at each subsequent view was compared with the total intensity of the junction at the time of initial saturation. *D*, example of a mouse neuromuscular junction that was viewed two times before (left) and after (right) continuous AChE blockade for 8 h with fasciculin 2-Alexa 594. The fluorescence intensity of AChE decreased significantly, indicating a decrease in AChE density. That the lost fluorescence was not recovered by fasciculin 2-Alexa 594 labeling implies that newly synthesized AChEs did not insert into the synaptic cleft. Scale bar, 20  $\mu\text{m}$ . *E*, graph summarizing percentage of the loss of AChEs obtained from many junctions during chronic blockade with fasciculin 2-Alexa 594 (blue line) and one-time blockade with Alexa fasciculin 2 (red line).

were saturated with fasciculin 2-Alexa 594/488, and superficial synapses were imaged, and then a high concentration of unlabeled fasciculin 2 (5–10-fold excess) or BW284C51 (10 mg/ml) was added continuously into the muscle. After 8 h, we found that  $94 \pm 5\%$  (S.D.,  $n = 60$ ) of the fluorescence intensity was lost from synapses. Surprisingly, however, when synapses in fixed tissue were labeled with biotin-fasciculin 2 followed with streptavidin Alexa 488/594 and then incubated with a high concentration of unlabeled fasciculin 2 (10-fold higher than biotin fasciculin 2) or BW284C51 (10 mg/ml), no evidence of fluorescence loss was observed during the same time period. Similarly, when fixed synapses were saturated first with unconjugated or conjugated fasciculin 2 (Alexa 488 or Alexa 594) and incubated over 8 h with a high concentration of fasciculin 2-Alexa 594 or Alexa 488, the loss of fasciculin 2 was negligible. These results indicate that unconjugated fasciculin 2 displaces conjugated fasciculin 2, but one conjugated fasciculin 2 does not displace another. Therefore, it is important to avoid using contaminated conjugated fasciculin 2 with unconjugated fasciculin 2.

We tested if changes of fluorescent fasciculin 2 in synapses *in situ* were due to bleaching. Synapses of fixed or live muscle were imaged and reimaged several times in succession using a water immersion objective

( $\times 20$  universal apochromate 0.7 numerical aperture), 25% light, and an exposure time of 100 ms. We found that there was no obvious loss of fluorescence intensity. This result excludes the possibility that bleaching is occurring under our imaging conditions. Altogether, these experiments indicate that fluorescent fasciculin 2 is an excellent probe to monitor AChE dynamics over time *in vivo*.

**Removal and Insertion of AChE from the Neuromuscular Junction in Vivo**—The loss of AChE from synapses was monitored over time following a single saturating dose of fluorescent fasciculin 2. Sternomastoid muscles from 10 mice were labeled one time with fasciculin 2-Alexa 594 (7  $\mu\text{g}/\text{ml}$ , 3 h) to saturate all AChEs. Superficial synapses were then imaged. The same synapses were relocated and reimaged one or multiple times over the next 7 days, and their fluorescence intensities were then measured using a quantitative fluorescence imaging assay. We found that 24 h after initial labeling, AChE fluorescence intensity was decreased by  $23 \pm 5\%$  (S.D.,  $n = 60$ ) (half-life of  $\sim 3$  days). This rate of loss slows over time; at 7 days,  $63 \pm 6\%$  (S.D.,  $n = 20$ ) of fluorescence intensity was lost, whereas fluorescence loss at the NMJs of fixed, labeled, and transplanted muscle was only about 15% over the same period (Fig. 2, *A–C*). Thus, the degradation of AChE from living syn-

apses is  $\sim 12$  days when corrected for fasciculin 2 unbinding. Similar results were found when the muscle was labeled with biotin-fasciculin 2, followed by a single saturating dose of Alexa 488/594 streptavidin. The removal rate of labeled AChE from the NMJ was nearly identical in the presence or absence of postsynaptic AChR blockade with  $\alpha$ -bungarotoxin. In addition, when the postsynaptic receptors were continuously blocked with  $\alpha$ -bungarotoxin, the loss of fluorescently labeled AChE over 8 h was comparable with loss of AChE in the absence of postsynaptic blockade, indicating that the removal of AChE from the synapse does not require postsynaptic activity.

Next we asked whether continuous AChE blockade affects its removal rate. To do this, the sternomastoid muscle was labeled with fasciculin 2-Alexa 594 to saturate all AChEs ( $7 \mu\text{g/ml}$ , 3 h). Superficial synapses were then imaged, and the same fasciculin 2-Alexa 594 was reapplied every 2 h for 8 h to ensure chronic AChE activity blockade; in this way, the continuous presence of fasciculin 2-Alexa 594 should result in the immediate blockade of any newly inserted AChEs). Because unconjugated fasciculin 2 and BW284C51 cause fasciculin 2-Alexa 594 displacement, we used only fasciculin 2-Alexa 594 to test the effect of chronic blockade on the net number of AChEs labeled with the same fluorescent fasciculin 2. Interestingly, junctions in which AChE was chronically blocked with fluorescent fasciculin 2 lost AChEs at a high rate of  $\sim 5\%/h$  for at least 8 h ( $65 \pm 6\%$  (S.D.,  $n = 34$ ) remained after chronic blockade;  $t_{1/2} = 12$  h) (Fig. 2, D and E). Thus, the net number of fluorescently labeled AChEs significantly decreased, indicating that lost AChE is not replaced by an equivalent addition of new AChE into the neuromuscular junction and also arguing against unbinding of fluorescent fasciculin 2 (see "Discussion").

Next we wanted to determine whether the AChEs removed from the synapses following saturation of the NMJ with fluorescent fasciculin 2 are replaced by newly inserted AChEs. To do this, AChEs in the sternomastoid muscle were saturated with fasciculin 2-Alexa 594, and fluorescence intensities at superficial synapses were measured. After 1–7 days, the same synapses were reimaged, and the loss of labeled AChE was determined. At each time point, the synapses were saturated again with the same fluorescent fasciculin 2 Alexa dye ( $7 \mu\text{g/ml}$ , 3 h) to label newly inserted AChEs and then reimaged, and their total fluorescence intensity was measured. We found that 1 day after initial labeling, AChE insertion nearly matches AChE loss (Fig. 3, A and B), and thereafter, the loss of AChE is compensated for by newly inserted AChE. These findings indicate that the removal and insertion of AChE are in equilibrium. These results are consistent with our previous findings in which preexisting AChEs were saturated with unconjugated fasciculin 2, and newly inserted AChE molecules were monitored over time by adding new fluorescent fasciculin 2 (19).

**Inhibition of AChE with Fasciculin 2 Increases the Rate of AChR Removal**—Given the effect of acetylcholine on nicotinic postsynaptic AChR gated ion channels, we next addressed whether inactivation of AChEs at the synaptic cleft affects the lifetime of postsynaptic membrane AChRs. To do this, we compared the loss rates of AChRs in the presence and absence of a single saturating dose of fasciculin 2. The sternomastoid muscle of four mice was labeled with a subsaturating dose of  $\alpha$ -bungarotoxin-Alexa 594 ( $5 \mu\text{g/ml}$ , 2 min) to ensure that the majority of AChRs were not occupied with  $\alpha$ -bungarotoxin and that synaptic transmission presumably remained functional. Under these labeling conditions, the AChR lifetime was previously shown to be long ( $t_{1/2} = 10$ –14 days) (23, 26). A single dose of unlabeled fasciculin 2 was then added to saturate and inactivate all AChEs ( $7 \mu\text{g/ml}$ , 3 h). The removal rate of AChRs was monitored over the next 3 days. AChR removal increased significantly ( $46 \pm 10\%$  (S.D.,  $n = 20$ ) fluorescence

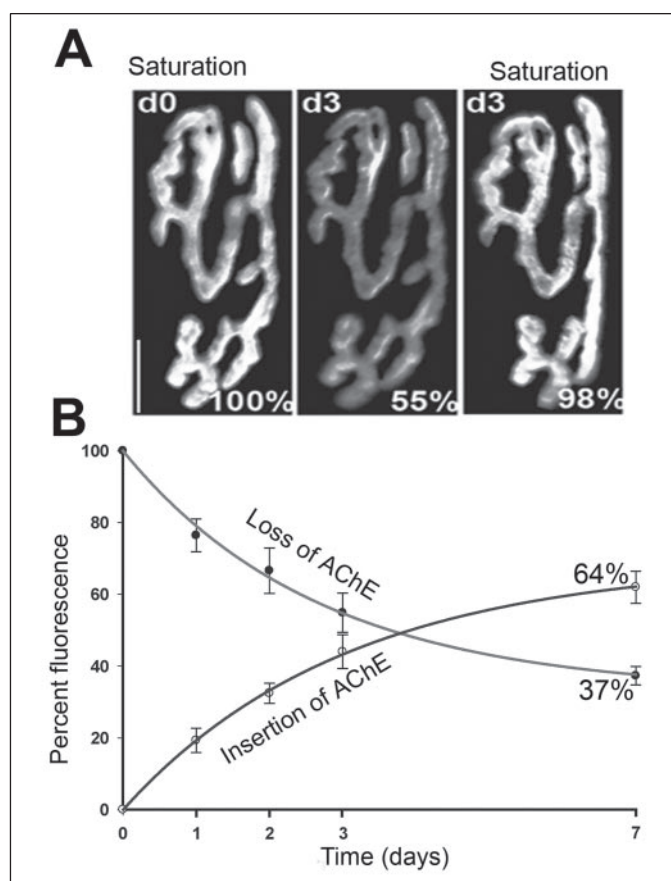


**FIGURE 3. Newly inserted AChEs matched the removal of AChEs.** A, example of a mouse neuromuscular junction that was saturated with fasciculin 2-Alexa 594 and was then saturated 3 days later with fresh fasciculin 2-Alexa 594 to determine the amount of new synaptic AChE insertion. B, graph summarizes results of AChE loss and insertion from 1–7 days later obtained from junctions with the approach shown in A. Note that nearly all lost AChEs were replaced by new AChE inserted into the NMJ at each data point.

intensity remaining after 3 days) compared with normal synapses ( $80 \pm 4.0\%$  (S.D.,  $n = 24$ ) fluorescence intensity remaining after 3 days) (Fig. 4A). This rapid AChR loss is accompanied by the appearance of small spots of fluorescence intensity beneath the plasmalemma (Fig. 4B).

**AChEs and AChRs Are Co-localized in the Same Internal Pool after Being Internalized**—To determine whether AChEs that have been lost from the NMJ are degraded locally in the synaptic cleft or if they are internalized into the muscle for degradation, we followed the fate of AChEs in innervated and denervated junctions in living adult mice. Because it would be difficult to detect AChE degradation product locally at the synaptic cleft, we took advantage of our observation that fluorescently labeled AChRs are internalized and degraded in the internal pool, identifiable as small bright spots of fluorescence in the perijunctional region of the NMJ (23, 30). If AChEs that are lost from synapses are internalized and degraded in the internal pool, then one would expect small spots of fluorescence inside the muscle fiber. Therefore, NMJs were doubly labeled with a single dose of (red) fasciculin 2-Alexa 594 to saturate AChEs and (green) bungarotoxin-Alexa 488 to label postsynaptic AChRs. When AChRs and AChEs labeled with distinct fluorophore conjugates were visualized 3 days later, a perfect co-localization of bright small spots of green and red fluorescent staining were observed in the same internal pool (Fig. 5, A–L). Quantification of AChE/AChR fluorescent spots revealed that more than 67% ( $n = 10$ ) were co-localized in the same internal vesicles (Figure 5L). These results were confirmed in denervated muscles that are known to undergo rapid receptor

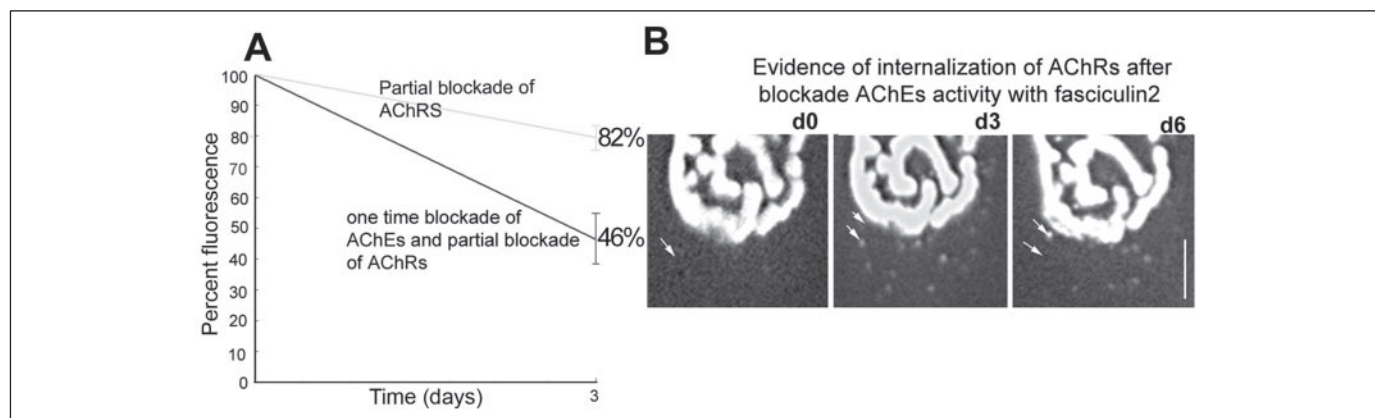


FIGURE 4. **Effect of AChE activity inhibition on AChR loss.** *A*, graph summarizing results of AChR loss from junctions labeled with a subsaturating dose of fluorescent bungarotoxin (under these conditions, the AChR loss rate is very slow ( $t_{1/2} = 10-14$  days (23)) and then labeled with one single saturating dose of fasciculin 2 to transiently block AChE activity. Note that receptors labeled with a low dose of bungarotoxin in the absence of fasciculin 2 were lost at a slow rate. *B*, three views of the same neuromuscular junction imaged over 6 days in a living mouse at high detector gain (the junctional branches are saturated). This muscle was labeled with a low dose of Alexa 594 bungarotoxin, and then AChE activity was blocked with a saturating dose of unlabeled fasciculin 2. At the time of labeling (*first panel*), no internalized spots of fluorescence are visible in the perijunctional region (see *arrow*). However, 3 days later (*second panel*), many internalized fluorescent spots appeared (see *arrows*). The position and the number of fluorescence changes over time (*third panel*) are shown, as indicated by *arrows*. Scale bar, 20  $\mu\text{m}$ .

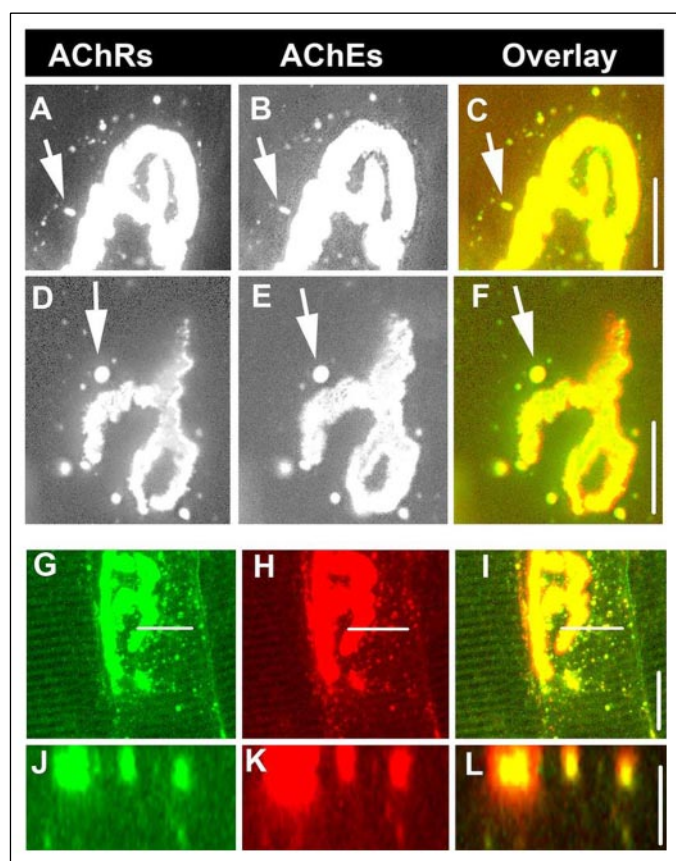


FIGURE 5. **Evidence for the internalization of AChE into the intracellular pool of the muscle fiber.** *A-C*, example of live innervated neuromuscular junction that was doubly labeled with single saturating doses of fasciculin 2-Alexa 594 (to label AChEs) and Alexa 488 bungarotoxin (to label AChRs) and imaged 3 days later. The gain was intentionally set high (the junctional branches are saturated) to show internalized fluorescent spots in the vicinity of the junction. As indicated by *arrows*, there is a perfect colocalization of AChEs and AChRs. Note that AChE visualization extends beyond the AChR labeling at the junction, as previously shown (46). *D-F*, example of an NMJ that was denervated 10 days prior to initial labeling. 3 days after Alexa 488 bungarotoxin (AChR) and fasciculin 2 Alexa 594 (AChE) labeling, large numbers of small bright internalized fluorescent spots corresponding to AChEs and AChRs are visible in the perijunctional region (see *arrows*). Scale bar, 40  $\mu\text{m}$ . *G-I*, confocal image (*z*-stack of 29 images) of a compressed fixed innervated NMJ that was previously labeled with Alexa 594 fasciculin 2 and Alexa 488 bungarotoxin. Note that nearly all spots of fluorescence (*red* and *green*) are localized in the same intracellular compartments. *J-L*, a single *z*-stack image shows that *red* and *green* signals co-localize intracellularly and not simply at different levels in the same vertical space. Scale bar, 20  $\mu\text{m}$ .

internalization. In muscle denervated 10 days earlier and bathed in fasciculin 2-Alexa 594 and bungarotoxin-Alexa 488 to label AChE and receptors, respectively, similar co-localized spots of green and red fluorescence ( $\sim 62\%$ ,  $n = 7$ ) were seen when synapses were reimaged 3 days after labeling (Fig. 5, *D-F*). These results suggest that a significant amount of AChEs are internalized before being degraded. *z*-Section of confocal images of muscles that were labeled 3–6 days with fasciculin 2-Alexa 594 (red) and bungarotoxin-Alexa 488 (green) prior to fixation showed in most cases a colocalization of green and red spots of fluorescence (Fig. 5, *J-L*).

## DISCUSSION

We have established that fluorescent fasciculin 2 specifically and selectively labels AChE with high affinity and thus can be used as a powerful tool to study the dynamics of AChE at the NMJ *in vivo*.

The rapid loss of fluorescent fasciculin 2 from synapses in living mice cannot be explained by diffusion of dissociated fasciculin 2 from pre-existing AChE but rather by AChE elimination. This idea is supported by the following results. 1) When fixed synapses were labeled with fasciculin 2-Alexa 594 at day 0 and the intensity of fluorescence was measured, there was a slow loss of fasciculin 2 even after 7 days. 2) When living NMJs were labeled with fasciculin 2 and treated with cycloheximide, there was only negligible fluorescence recovery when new fluorescent fasciculin 2 was added (19). 3) When AChEs were continuously blocked with the same fluorescent fasciculin 2-Alexa dye, the loss of fluorescence significantly increased, indicating that fluorescence loss cannot be due to unbinding of fasciculin 2 from synapses (Fig. 2, *D* and *E*). If unbinding of fasciculin 2 did occur, one would expect that the net fluorescence intensity at each synapse over the time window of the experiment would remain unchanged as each unbound fluorescent fasciculin 2 would be replaced by another fluorescent fasciculin 2 present in the neck of the mouse.

In contrast to previous studies, where the half-life of fasciculin 2 unbinding from AChE in the test tube ranges from 1 to 6 h (14, 15, 37), our studies argue that the half-life at synapses in fixed and living mouse muscle is far slower (several days). This discrepancy could potentially be explained by the high concentration of AChE at the neuromuscular junction (in the range of 0.2 mM, around 2500 molecules/ $\mu\text{m}^2$ ) (18, 31). Therefore, a single fasciculin 2 molecule might bind and rebind many times before escaping the synapse, thus producing an apparent unbinding rate much slower than the actual rate of dissociation of the molec-

ular complex. Although our results suggest that rebinding is not a major problem, further investigations are still needed. At the neuromuscular junction, AChE is organized into tetramers and associated with several other proteins. Thus, it seems possible that when AChEs are extracted from their native milieu, they are altered in a way that greatly decreases their affinity for fasciculin 2. Consistent with this idea, previous studies have shown that embryonic monomeric rat brain AChE is more poorly inhibited by fasciculin than tetrameric rat brain AChE (32).

One unexpected finding is that fluorescent conjugated fasciculin 2 can be displaced from AChE in fixed and living synapses by unconjugated fasciculin 2 or BW284C51. However, when biotin-fasciculin 2 was used to label AChE followed by streptavidin, unconjugated fasciculin 2 or BW284C51 is unable to displace biotin-fasciculin 2 from AChE at synapses, and the reason for the nonreciprocal displacement is unclear at present and needs further experiments.

Using fluorescent toxin as a probe, our results indicate that the half-life of AChE after a one-time blockade with fasciculin 2 is fast initially (around 3 days) and slow later (half-life of more than 12 days). The difference in half-life between our results and previous studies might be attributed to experimental conditions as well as the use of probes. In previous studies in which DFP was used as a probe, the AChE lifetime was estimated to be fixed at a  $t_{1/2}$  of ~20 days (13). In these experiments, inhibition of AChE was always followed by nerve stimulation to monitor muscle contraction and ensure that all AChEs were inhibited with DFP. This procedure could generate a local necrosis in the postsynaptic site, which may delay the insertion of new AChE (13). In addition, DFP is considered to be a nonspecific inhibitor that blocks a range of esterases, including AChE, butyrylcholinesterase, serine proteases, and lipases, which may affect the physiology of the NMJ. DFP labeling also results in high background, which makes the detection of low synaptic AChE density impossible to study. Finally, the DFP labeling procedure *per se*, which involves a complex sequence of inhibition and reactivation steps that allow detection of DFP sites by electron microscopy using a very long exposure time (months), could be a potential source for a lack of sensitivity (18).

By contrast with studies using DFP, the use of fluorescent fasciculin 2 is highly specific to AChE (19), and more importantly, the comparison of fluorescence loss was assayed from the same NMJ imaged over time. In addition, under our labeling conditions with fluorescent fasciculin 2, the nerve was never being stimulated, which may explain the lack of any obvious postsynaptic necrosis. Although unlikely, it is worth mentioning that AChE dynamics might be affected by fasciculin 2 being internalized alone into the cell over time. Altogether, these differences may explain the discrepancies between our results and previous reports in which the fast dynamics of AChE was not revealed.

The rate at which inactivated AChEs are lost from junctions after a one time complete blockade with fasciculin 2 is complicated. These AChE loss rates could correspond to at least two populations of AChE in the junction: one that turns over rapidly and one that turns over very slowly. It has been demonstrated that part of the ColQ-AChE complex is covalently associated in the basal lamina, and it thus seems likely that this enzyme represents a very stable pool of AChE, whereas the non-linked complex may be more dynamic. To date, the proportion of this covalently linked ColQ-AChE is debated, so it may represent the majority of the enzyme (33) or only a minor proportion (34). From our quantification, we estimate that approximately one-third of the AChEs could be very stable, since the labeling could be found weeks after initial saturation.

On the other hand, our results argue that when AChEs are continuously inactivated with fluorescent fasciculin 2, the AChE loss is

increased and is not compensated by a significant increase in insertion of new AChE. This raises the question of how AChE activity blockade may affect the insertion of newly synthesized AChEs into the synaptic cleft. One possibility would be that transient interactions of the catalytic subunit of AChE might participate directly in its accumulation in the synaptic cleft. Several lines of evidence suggest that AChE may interact with unknown partners through the peripheral anionic site (for a review, see Ref. 35). Because fasciculin 2 masks the active site of the molecule (36), AChE accumulation in the NMJ might be affected. Since both heparin binding sites and the C-terminal domain of ColQ are necessary for AChE clustering (11), it is possible that the catalytic domain may also participate in AChE accumulation. In support of this idea is the finding that during development, AChE and butyrylcholinesterase are both clustered by ColQ but do not have the same dynamic after denervation (37). Alternatively, AChE expression could be depressed by an unknown signal from the muscle, the nerve, or both that is possibly dependent upon an excess of acetylcholine.

The observation that the blockade of AChE activity with fasciculin 2 increases the loss rate of AChR from the postsynaptic membrane raises the idea that the ratio between AChE activity and AChR is crucial for a properly functioning synapse. It is clear that inhibition of AChE activity increases acetylcholine accumulation in the synaptic cleft, which might cause repeated activation of the nicotinic acetylcholine receptor. This repetitive activation can rapidly change the three-dimensional structure of the AChR to a desensitized nonconducting conformation within seconds (38, 39). Thus, persistent AChR desensitization would block synaptic transmission and contribute significantly to the paralysis of skeletal muscle (40). Also, excess activation of these receptors may raise the intracellular calcium concentration to pathological levels (41), although no obvious myopathy was observed in our experiments. Consistent with this, recent work showed that AChE or ColQ mutant mice exhibit few molecules of AChRs at synapses (42), and a recent finding also showed that acetylcholine is able to cause the dispersion of receptors (43, 44). In this scheme, it would be very informative to evaluate the dynamics of AChR in the absence of AChE activity and to analyze the signaling pathway involved in this regulation.

One intriguing result in this work is the colocalization of AChR and AChE in the same internal compartment. At the neuromuscular junction, AChE is organized in tetramers that are tethered through a collagen tail (ColQ) to the extracellular matrix. Whereas the cellular mechanisms by which AChEs are removed from synapses are not known, one possibility is that AChEs and AChRs are endocytosed separately through distinct internalization mechanisms and then fuse once they are in an internal pool. The fact that small spots of fluorescence are found near the junction (Fig. 5) might suggest that the perijunctional region may serve as the site of internalization, and AChEs may only be degraded after they have moved to this space. Indeed, lateral movement of AChE was previously reported during development (45) and in cultured cells (4), suggesting that the ColQ-AChE complex could be dynamic despite its size and its multiple interactions with other proteins. We cannot exclude the possibility that AChEs and AChRs are internalized locally directly under the NMJ.

*Acknowledgments*—We thank Drs. Zoran Radic and Terry Rosenberry and the members of our laboratory for helpful discussions and Dr. Richard Hume, Amy Chang, and Robert Denver for critical comments.

## REFERENCES

1. Katz, B., and Miledi, R. (1973) *J. Physiol.* **231**, 549–574
2. Krejci, E., Thomine, S., Boschetti, N., Legay, C., Sketelj, J., and Massoulié, J. (1997)

- J. Biol. Chem.* **272**, 22840–22847
3. Deprez, P., Inestrosa, N. C., and Krejci, E. (2003) *J. Biol. Chem.* **278**, 23233–23242
  4. Peng, H. B., Xie, H., Rossi, S. G., and Rotundo, R. L. (1999) *J. Cell Biol.* **145**, 911–921
  5. Arikawa-Hirasawa, E., Rossi, S. G., Rotundo, R. L., and Yamada, Y. (2002) *Nat. Neurosci.* **5**, 119–123
  6. Cote, P. D., Moukhles, H., Lindenbaum, M., and Carbonetto, S. (1999) *Nat. Genet.* **23**, 338–342
  7. Jacobson, C., Cote, P., Rossi, S., Rotundo, R., and Carbonetto, S. (2001) *J. Cell Biol.* **152**, 435–450
  8. Costell, M., Gustafsson, E., Aszodi, A., Morgelin, M., Bloch, W., Hunziker, E., Ad-dicks, K., Timpl, R., and Fassler, R. (1999) *J. Cell Biol.* **147**, 1109–1122
  9. Feng, G., Krejci, E., Molgo, J., Cunningham, J. M., Massoulié, J., and Sanes, J. R. (1999) *J. Cell Biol.* **144**, 1349–1360
  10. Kimbell, L. M., Ohno, K., Engel, A. G., and Rotundo, R. L. (2004) *J. Biol. Chem.* **279**, 10997–11005
  11. Cartaud, A., Strohlic, L., Guerra, M., Blanchard, B., Lambergeon, M., Krejci, E., Cartaud, J., and Legay, C. (2004) *J. Cell Biol.* **165**, 505–515
  12. Salpeter, M. M., Kasprzak, H., Feng, H., and Fertuck, H. (1979) *J. Neurocytol.* **8**, 95–115
  13. Kasprzak, H., and Salpeter, M. M. (1985) *J. Neurosci.* **5**, 951–955
  14. Karlsson, E., Mbugua, P. M., and Rodriguez-Ithurralde, D. (1984) *J. Physiol. (Paris)* **79**, 232–240
  15. Karlsson, E., Mbugua, P. M., and Rodriguez-Ithurralde, D. (1985) *Pharmacol. Ther.* **30**, 259–276
  16. Menez, A. (1998) *Toxicol.* **36**, 1557–1572
  17. Marchot, P., Khelif, A., Ji, Y. H., Mansuelle, P., and Bougis, P. E. (1993) *J. Biol. Chem.* **268**, 12458–12467
  18. Anglister, L., Eichler, J., Szabo, M., Haesaert, B., and Salpeter, M. M. (1998) *J. Neurosci. Methods* **81**, 63–71
  19. Martinez-Pena y Valenzuela, I., Hume, R. I., Krejci, E., and Akaaboune, M. (2005) *J. Biol. Chem.* **280**, 31801–31808
  20. Panchuk-Voloshina, N., Haugland, R. P., Bishop-Stewart, J., Bhalgat, M. K., Millard, P. J., Mao, F., Leung, W. Y., and Haugland, R. P. (1999) *J. Histochem. Cytochem.* **47**, 1179–1188
  21. Lichtman, J. W., Magrassi, L., and Purves, D. (1987) *J. Neurosci.* **7**, 1215–1222
  22. Turney, S. G., Culican, S. M., and Lichtman, J. W. (1996) *J. Neurosci. Methods* **64**, 199–208
  23. Akaaboune, M., Culican, S. M., Turney, S. G., and Lichtman, J. W. (1999) *Science* **286**, 503–507
  24. Duxson, M. J. (1982) *J. Neurocytol.* **11**, 395–408
  25. Balice-Gordon, R. J., and Lichtman, J. W. (1994) *Nature* **372**, 519–524
  26. Akaaboune, M., Grady, R. M., Turney, S., Sanes, J. R., and Lichtman, J. W. (2002) *Neuron* **34**, 865–876
  27. Andreose, J. S., Xu, R., Lomo, T., Salpeter, M. M., and Fumagalli, G. (1993) *J. Neurosci.* **13**, 3433–3438
  28. Nguyen-Huu, T., Dobbertin, A., Barbier, J., Minic, J., Krejci, E., Duvaldestin, P., and Molgo, J. (2005) *Anesthesiology* **103**, 788–795
  29. Eastman, J., Wilson, E. J., Cervenansky, C., and Rosenberry, T. L. (1995) *J. Biol. Chem.* **270**, 19694–19701
  30. Bruneau, E., Sutter, D., Hume, R. I., and Akaaboune, M. (2005) *J. Neurosci.* **25**, 9949–9959
  31. Salpeter, M. M., Rogers, A. W., Kasprzak, H., and McHenry, F. A. (1978) *J. Cell Biol.* **78**, 274–285
  32. Moreno, R. D., Campos, F. O., Dajas, F., and Inestrosa, N. C. (1998) *Int. J. Dev. Neurosci.* **16**, 123–134
  33. Rossi, S. G., and Rotundo, R. L. (1993) *J. Biol. Chem.* **268**, 19152–19159
  34. Casanueva, O. I., Garcia-Huidobro, T., Campos, E. O., Aldunate, R., Garrido, J., and Inestrosa, N. C. (1998) *J. Biol. Chem.* **273**, 4258–4265
  35. Soreq, H., and Seidman, S. (2001) *Nat. Rev. Neurosci.* **2**, 294–302
  36. Bourne, Y., Taylor, P., and Marchot, P. (1995) *Cell* **83**, 503–512
  37. Berman, H. A., Decker, M. M., and Jo, S. (1987) *Dev. Biol.* **120**, 154–161
  38. Katz, B., and Thesleff, S. (1957) *J. Physiol.* **138**, 63–80
  39. Katz, E. J., Cortes, V. L., Eldefrawi, M. E., and Eldefrawi, A. T. (1997) *Toxicol. Appl. Pharmacol.* **146**, 227–236
  40. Thesleff, S. (1955) *Nature* **175**, 594–595
  41. Leonard, J. P., and Salpeter, M. M. (1979) *J. Cell Biol.* **82**, 811–819
  42. Adler, M., Manley, H. A., Purcell, A. L., Deshpande, S. S., Hamilton, T. A., Kan, R. K., Oyler, G., Lockridge, O., Duysen, E. G., and Sheridan, R. E. (2004) *Muscle Nerve* **30**, 317–327
  43. Lin, W., Dominguez, B., Yang, J., Aryal, P., Brandon, E. P., Gage, F. H., and Lee, K. F. (2005) *Neuron* **46**, 569–579
  44. Misgeld, T., Kummer, T. T., Lichtman, J. W., and Sanes, J. R. (2005) *Proc. Natl. Acad. Sci. U. S. A.* **102**, 11088–11093
  45. Ziskind-Conhaim, L., Inestrosa, N. C., and Hall, Z. W. (1984) *Dev. Biol.* **103**, 369–377
  46. Rotundo, R. L. (2003) *J. Neurocytol.* **32**, 743–766